*Proc. Natl. Acad. Sci. USA*
Vol. 86, pp. 2918–2922, April 1989
Neurobiology

# Voltage dependence of adaptation and active bundle movement in bullfrog saccular hair cells

(mechanoreceptor/vestibular system/ion channel/cell motility)

JOHN A. ASSAD*†, NIR HACOHEN*, AND DAVID P. COREY*‡

*Neuroscience Group, Howard Hughes Medical Institute, and Department of Neurology, Wellman 4, Massachusetts General Hospital, Fruit Street, Boston, MA 02114; and †Department of Neurobiology and ‡Program in Neuroscience, Harvard Medical School, Boston, MA 02115

*Communicated by Charles F. Stevens, January 3, 1989*

ABSTRACT **Hair cells of the bullfrog sacculus adapt to maintained displacement stimuli in a manner that suggests an active regulation of the tension stimulus reaching transduction channels. We have examined adaptation in dissociated hair cells by whole-cell patch-clamp recording and video microscopy. Adaptation was present in these cells, and it depended on extracellular calcium. The adaptation rate—as well as the position of the resting current–displacement curve—also depended on membrane potential, suggesting that calcium passes into the cytoplasm to reach its site of action. After abrupt hyperpolarization, the adaptation rate increased within milliseconds, suggesting that the calcium site is within a few micrometers of the ion channels through which calcium enters. The voltage dependence of the resting current–displacement curve, together with the "gating springs" hypothesis for transduction, predicts movement of the bundle away from the kinocilium when the cell is depolarized. This was observed.**

The bullfrog sacculus is exquisitely sensitive to linear acceleration: vibratory accelerations of only 1 $mm \cdot s^{-2}$ saturate the output of the organ (1). Yet the static acceleration of gravity is 4 orders of magnitude greater. In fact, the receptor cells of the sacculus possess an extraordinary feedback mechanism—adaptation—which shifts the sensitive range of the cells within tens of milliseconds so as to cancel static biases. Adaptation has been studied most extensively by *in vitro* microphonic recording from the bullfrog sacculus (2, 3). In these experiments, which measure the receptor current of several hundred hair cells stimulated *en masse*, a maintained displacement of the stereociliary bundles elicits a transduction current, which declines to a steady level in ≈100 ms. This decrement in current is not an inactivation process; rather, it is due to a shift in the relation between bundle displacement and receptor current—the $I(X)$ curve—in the direction of the adapting step. If bundle displacement directly communicates tension to the transduction channels (4), then adaptation in response to positive displacements (toward the kinocilium) must act to relax the mechanical input, favoring reclosure of the channels, while adaptation to negative stimuli (away from the kinocilium) restores tension, favoring reopening. In fact, positive displacements produce a mechanical relaxation, which can be directly observed as an increase in bundle compliance with the same time course as adaptation (5).

Little is known of the cellular mechanism of adaptation. Higher extracellular calcium increases the rate of adaptation to both positive and negative stimuli and shifts the resting $I(X)$ curve so there are fewer channels open at rest (3, 6). In this study, we have examined the effects of membrane potential and extracellular calcium concentration on adaptation in single isolated hair cells from the bullfrog sacculus to localize the specific site of action of calcium. The results are consistent with a calcium site very near the transduction channels. They also predict a voltage-dependent bundle movement, which was observed with video microscopy. A preliminary report of this work has appeared (7).

The publication costs of this article were defrayed in part by page charge payment. This article must therefore be hereby marked "*advertisement*" in accordance with 18 U.S.C. §1734 solely to indicate this fact.

## MATERIALS AND METHODS

**Preparation.** Saccular hair cells from adult bullfrogs (*Rana catesbeiana*) were dissociated following a procedure modified from Lewis and Hudspeth (8). Sacculi were exposed, and an oxygenated papain solution [0.5 mg of papain per ml (Calbiochem) and 2.5 mM L-cysteine] was dripped into the perilymphatic space for 30 min at room temperature; this procedure and all subsequent steps of the dissociation were done in a low-calcium saline containing 120 mM Na, 2 mM K, 0.1 mM Ca, 122 mM Cl, 3 mM dextrose, and 5 mM Hepes (pH 7.25). After a 1-min wash with bovine serum albumin (0.5 mg/ml) (Sigma), maculae were dissected from the frog into a dish and incubated for 30 min in bacterial protease type XXIV (50 μg/ml) (Sigma) to loosen the overlying otolithic membranes. Single cells were dissociated from the maculae with an eyelash and settled onto the clean glass bottom of the recording chamber. This procedure, in which papain was largely prevented from reaching the mechanically sensitive hair bundles by tight junctions between hair cells and supporting cells, resulted in a substantially higher proportion of transducing cells and larger transduction currents than with other protocols (8, 9).

**Mechanical Stimulation.** Mechanical displacements were delivered to the stereociliary bundle using a stiff glass probe driven by a two-dimensional piezoelectric bimorph stimulator that moved in the horizontal plane (10). The probe tip adhered directly to the kinociliary bulb; a photodiode provided an optical monitor of probe movement near its attachment to the bundle. In addition, the stimulus probe and attached stereociliary bundle were directly observed at high magnification (×10,000) with an analog-enhanced video camera system (Hamamatsu C2400) to assess the relative motion of the bundle and cell body.

**Electrical Recording.** Membrane currents were recorded by whole-cell patch-clamp recording (11, 12) with micropipettes attached to the basolateral membrane of the cell near the cuticular plate. Seals on this surface proved extremely stable: initial seal resistances were typically 20–50 GΩ, and it was not uncommon to record from a cell for >30 min. Currents were recorded with a Yale Mk.V patch-clamp amplifier equipped with a 1-GΩ head stage. When necessary, leakage, capacitive, and voltage-dependent currents were subtracted by presenting voltage steps with and without mechanical stimulation. Leakage currents at −80 mV were typically −100 pA. Residual series resistance after compensation was usually 6–8 MΩ. The current signal and photodiode signal were filtered at 5 kHz and digitized on-line with a PDP-11/73 computer system (Indec Systems, Sunnyvale, CA); the

computer also generated the command voltage and mechanical stimulator signals.

**Video Recording.** The image of the hair bundle was recorded onto videotape and transferred to optical memory disc for analysis. To determine what part of the cell was moving, single frames acquired at +80 and −80 mV were subtracted and the contrast was enhanced 15-fold with an image processor (Imaging Technology 151).

**Solutions.** Electrodes were filled with an internal solution containing 120 mM Cs, 47 mM Cl, 43 mM F, 2 mM Mg, 10 mM EDTA or EGTA, and 5 mM Hepes (pH 7.25). The recording chamber was continually perfused with an oxygenated room-temperature bath solution containing 120 mM Na, 4 mM Ca, 2 mM K, 128 mM Cl, 3 mM dextrose, and 5 mM Hepes. In some experiments, a low-calcium solution (125.6 mM Na, 0.1 mM Ca, 2 mM K, 3 mM dextrose, and 5 mM Hepes) was puffed from a second pipette onto the cell with a solenoid-controlled pressure pulse. The puffer pipette (tip diameter, 1 μm) was positioned 20–30 μm from the stereociliary bundle; outflow was visualized with phenol red in control experiments.

## RESULTS

**The Current–Displacement Relation.** Dissociated hair cells were responsive to mechanical stimuli: maximal inward transduction currents were typically 50–300 pA in response to positive displacements at a holding potential of −80 mV. Fig. 1*A* illustrates the responses to a triangle-wave displacement of the hair bundle. Positive displacements (toward the kinocilium) elicited an inward current, which saturated with increasing displacement, while negative displacements turned off a resting inward current. The transduction current was plotted against bundle displacement to generate a current–displacement [$I(X)$] curve (Fig. 1*B*). A striking feature of the sigmoidal $I(X)$ curve was a pronounced negative hysteresis: the $I(X)$ curves corresponding to increasing or decreasing half cycles of the stimulus were shifted along the displacement axis relative to one another. Adaptation, which causes a positive shift in response to positive displacements, is expected to produce this effect. Maintained step displacements produced an adaptation-like decline in the response as well (Fig. 1*C*). The $I(X)$ curve from step displacements (Fig. 1*D*) was fairly well fit by a two-state Boltzmann relation, and its steepness was comparable to that reported previously (refs. 2 and 14; but see ref. 13).

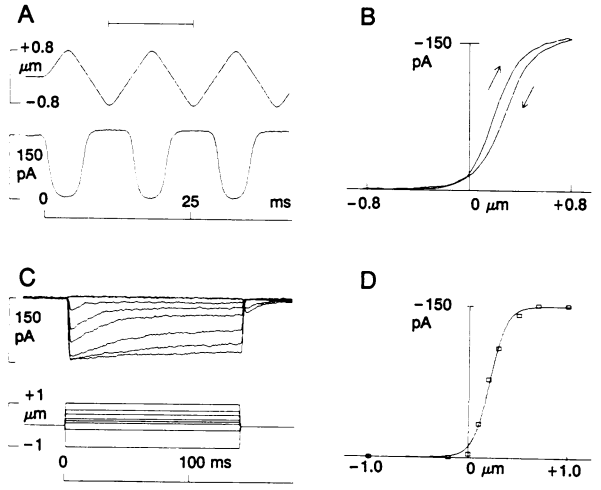


FIG. 1. Responses of hair cells to oscillatory or step displacements of their hair bundles. (*A*) Response to a 70-Hz triangle-wave stimulus (top trace). (*B*) $I(X)$ curve generated by plotting receptor current against an optical recording of stimulus-probe displacement over the middle cycle (horizontal bar in *A*). (*C*) Response to a family of step displacements. (*D*) The $I(X)$ curve generated by plotting the initial values of current (before adaptation occurred) against displacement steps. The steepness was 7.8 kcal·mol$^{-1}$·μm$^{-1}$ (1 cal = 4.184 J), equivalent to 54 fN (13). In 21 cells, the average steepness of $I(X)$ curves measured by step displacements was 49 ± 16 fN (mean ± SD). Note that in *B* and *D*, inward (negative) receptor current is shown as upward to facilitate comparison with channel open probability.

**Potential Artifacts.** These observations indicated that the adaptation mechanism was preserved in the dissociated patch-clamped cells. Yet several artifacts could also have produced the results. One such problem is poor adhesion of the cell to the substrate: if the cell body were to move over tens of milliseconds after mechanical stimulation, the net stimulus to the bundle would be diminished, producing a decline in the transduction current that might mimic adaptation. However, high-resolution video imaging of bundle displacements in most cases revealed neither movement of the soma nor slippage of the stimulus probe. Only those cells that showed no perceptible (<0.1 μm) movement of the soma were used for this study.

It was also essential to distinguish between adaptation—a shift in the $I(X)$ relationship that indicates relaxation of the effective stimulus—and channel inactivation. For Fig. 2, instantaneous $I(X)$ curves were generated by delivering a series of test steps at three time points during a 0.7-μm displacement lasting 100 ms. During the maintained stimulus, the $I(X)$ curve moved rightward along the displacement axis, following a roughly exponential time course. Thus, the transduction current did not inactivate—there was no decrement in the peak-to-peak current—rather, it declined be-

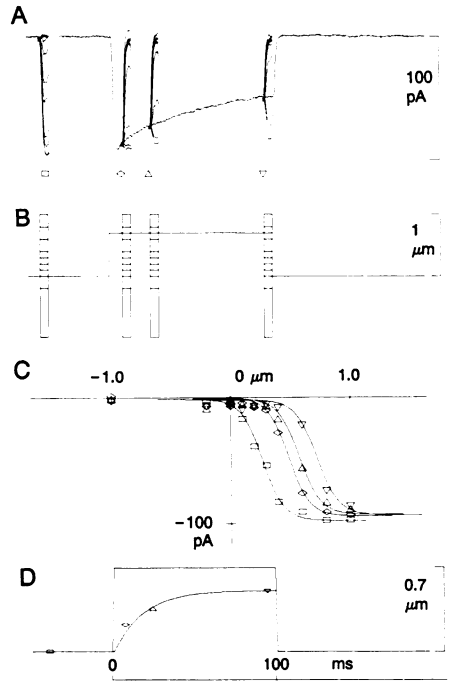


FIG. 2. Shift of the $I(X)$ curve during a maintained displacement at −80 mV. (*A*) Superimposed responses to 10 stimulus presentations. (*B*) The stimulus consisted in each case of a maintained displacement of 0.7 μm for 100 ms and one short test step of varying amplitude and temporal position. (*C*) $I(X)$ curves obtained by plotting the responses to test steps shifted during the maintained displacement. (*D*) The amplitude of the shift was measured at the midpoint of the sigmoidal curves and plotted against time. The time constant of the shift was 17.4 ms; in 10 cells, the average time constant was 13.8 ± 5.7 ms, similar to that measured in other preparations of the bullfrog sacculus (3). Because the displacement was near the saturated portion of the $I(X)$ curve, the decline in current (*A*) was slower than the actual time course of the $I(X)$ curve shift (*D*).

cause the $I(X)$ curve shifted so that fewer channels were open. This experiment argued as well against a third possible artifact: activation of a slowly developing outward current that summed with the transduction current. An outward current would have shifted the $I(X)$ curve upward along the current axis. No such vertical offset was observed.

**Dependence on Calcium and Membrane Potential.** As in the *in vitro* microphonic preparation (3), the rate of adaptation was sensitive to the concentration of extracellular calcium. In the experiment of Fig. 3*A*, the hair cell was maintained in a bath solution containing 4 mM calcium. Bundle displacement elicited a transduction current that declined during the step. When the stereociliary bundle was then superfused by applying slight positive pressure to a micropipette containing a 0.1 mM calcium solution, the same displacement produced a more slowly declining current. Furthermore, the amount of negative hysteresis in $I(X)$ curves obtained from triangle-wave stimulation was greater in 4 mM than in 0.1 mM external calcium (see below).

These results do not distinguish between an extra- or intracellular site for the action of calcium, since calcium can enter the stereocilia through transduction channels (9, 15). However, if the site is intracellular, the rate of adaptation should be sensitive to membrane potential, since calcium flux through open transduction channels should be voltage dependent. Although the current–voltage relation for calcium in physiological saline is not known, simple models for ion permeation predict an $e$-fold increase in influx for each 20–50 mV of hyperpolarization (16). On the other hand, calcium binding to a site located outside the membrane's electric field should be unaffected by membrane potential. In fact, the adaptation rate was voltage dependent. In the experiment shown in Fig. 3*B*, the same 0.7-$\mu$m step displacement was delivered to a cell held between −110 and +90 mV. The decline in current was quite pronounced at the negative holding potentials, but it was virtually absent at +60 and +90 mV.

For the most part, procedures that reduce the adaptation rate to positive displacements (such as lowering calcium) appear to increase the tension in the putative "gating springs." That is, they shift the resting curve toward the left

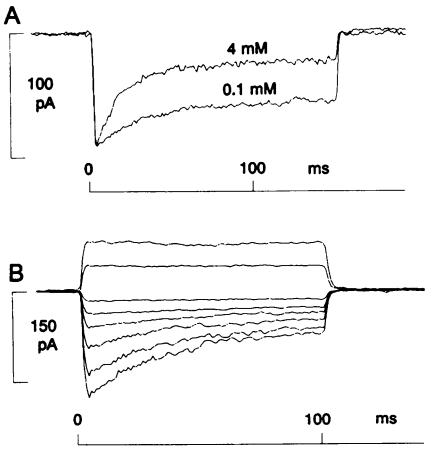


FIG. 3. Calcium and voltage dependence of adaptation. (*A*) The decline in the current, indicating the rate of adaptation, was greater in high (4 mM) than in low (0.1 mM) calcium saline (0.5-$\mu$m displacement). High calcium produced a partial block of the transduction current; accordingly, the trace in 4 mM calcium was scaled to match the peak current in 0.1 mM calcium. (*B*) The decline was also faster at hyperpolarized potentials. Membrane potential was changed to a new value 300 ms before the mechanical stimulus (0.7-$\mu$m displacement) and held for the duration of the trace. Test potentials (from top trace down) were as follows: +90, +60, +10, −10, −30, −60, −90, and −110 mV. Traces were aligned so that resting currents at each potential were superimposed.

so that more channels are open at rest (6). Fig. 4 illustrates that depolarization, which reduced adaptation (Fig. 3), also shifted the position of the resting $I(X)$ curve toward the left. The $I(X)$ curves were generated by a series of 5-ms step displacements, with the holding potential alternated between +80 and −80 mV. At −80 mV, the transduction current was nearly 0 at rest, but at +80 mV, the $I(X)$ curve was shifted left along the displacement axis so that 42% of the channels were open at rest. Changing the membrane potential resulted in more than a simple shift, however: $I(X)$ curves generated at −80 mV were consistently steeper than those measured at +80 mV (see *Discussion*).

The voltage dependence of the $I(X)$ curve immediately presents a potential artifact: since the $I(X)$ curve is sigmoidal, the same mechanical displacement may be saturating at +80 mV, but not −80 mV, so that at +80 mV the same rate of adaptive shift—along the displacement axis—would produce a slower decline in current. Similarly, the shallower slope of the $I(X)$ curve at +80 mV would produce a slower decline. However, two observations argue strongly against this possibility. First, there was a pronounced negative hysteresis in $I(X)$ curves derived from triangle-wave stimulation at −80 mV, but not +80 mV, and there was no current decline for small nonsaturating steps at +80 mV (data not shown).

The voltage dependence of adaptation is consistent with, but does not prove, the hypothesis that calcium is acting at an intracellular site. It is conceivable that the adaptation mechanism is intrinsically voltage dependent: perhaps some element of the adaptation machinery spans the membrane and is able to sense membrane potential. However, another experiment shows that the voltage dependence requires the presence of extracellular calcium. In Fig. 5, the $I(X)$ curves were derived from triangle-wave stimuli, with the holding potential alternated between +80 and −80 mV. In 4 mM external calcium, there was a pronounced negative hysteresis due to adaptation at −80 mV, but not +80 mV, and the $I(X)$ curve at +80 mV was shifted to the left. Yet, in hair cells bathed in low external calcium (0.1 mM), hysteresis was limited and the voltage dependence of the resting $I(X)$ curve was less marked. This suggests that the voltage dependence of adaptation and of the $I(X)$ curve are indirect consequences of calcium entry through ion channels.

**Spatial Localization of the Action of Calcium.** The only calcium-permeable channels known in hair cells that are open at −80 mV are the transduction channels themselves (17), located at the tips of stereocilia (18). If calcium must enter the stereocilia through transduction channels to reach its site of action, we can localize the site—and presumably the mechanism itself—by measuring how rapidly calcium reaches that site. Control of membrane potential offered a rapid way to change calcium entry. Fig. 6 illustrates an experiment in which a hair cell was bathed in a high calcium saline. When

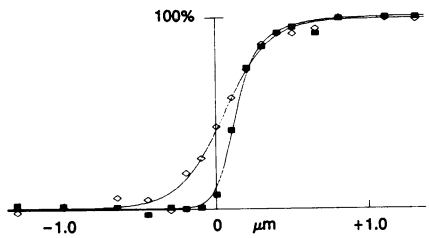


FIG. 4. Voltage dependence of the resting $I(X)$ curve. Currents are shown as a percentage of the maximal response. At −80 mV (■), 9% of the channels were open at rest; steepness, 47 fN. At +80 mV (◇), 42% of the channels were open at rest; steepness, 30 fN. The $I(X)$ curve at −80 mV was steeper than at +80 mV in all seven cells measured in this manner: the average steepness was 48 ± 19 fN at −80 mV and 32 ± 17 fN at +80 mV. The percent of channels open at rest was 10% ± 7% at −80 mV and 45% ± 17% at +80 mV.

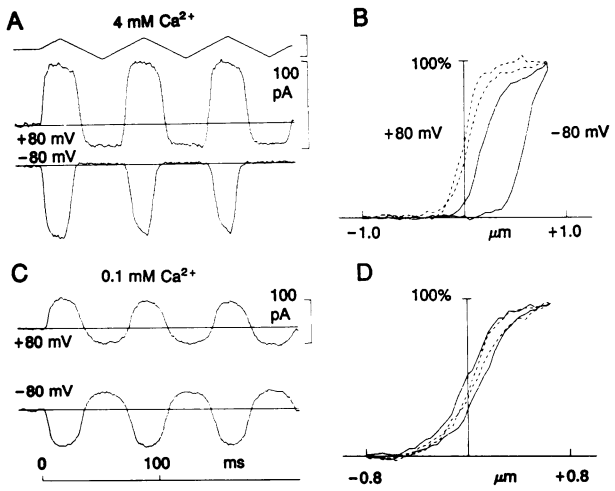


FIG. 5. The responses to a triangle-wave stimulus were plotted against an optical recording of the stimulus-probe movement to yield normalized $I(X)$ curves. (*A* and *B*) Calcium in bath (4 mM) (solid curve, −80 mV; dashed curve, +80 mV). For 35 cells, the average shift with depolarization in 4 mM calcium was 346 ± 117 nm. (*C* and *D*) Calcium (0.1 mM); different cell than in *A*. In seven cells in 0.1 mM calcium, the average shift with depolarization was 77 ± 47 nm. Stimulus amplitude: *A*, 1 μm; *C*, 0.8 μm. It was difficult to obtain an accurate measure of the steepness of $I(X)$ curves using triangle-wave stimuli, because adaptation was occurring continuously during the displacement.

the membrane potential was held at +90 mV there was little adaptation following a displacement step, but the adaptation rate abruptly increased (within 1–2 ms) when the cell was then hyperpolarized to −90 mV.

How far can calcium diffuse in 2 ms? We calculated the time course of intracellular calcium diffusion from the tip of a stereocilium, assuming a diffusion constant the same as in water and assuming no buffering within the stereocilium. The calculation thus represents a probable upper limit for distance. The result (Fig. 6, bottom trace) indicates that, after a step change in membrane potential, calcium increases rapidly

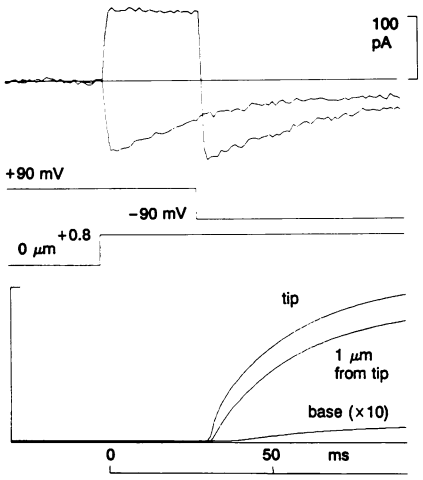


FIG. 6. Time course of calcium action. Membrane potential was held at +90 mV for 300 ms preceding a 0.5-μm stimulus and then changed to −90 mV, 30 ms after the start of the mechanical stimulus. Membrane potential was held continuously at −90 mV in the control trace. The time course of intracellular calcium concentration change predicted from a simple diffusion model is shown in the bottom trace for the tip of a stereocilium, 1 μm from the tip, and at the base (where it is expanded by a factor of 10). The concentration axis in this trace is arbitrary, because the relative permeability of calcium is not known (9, 15) and because the exact voltage dependence of the permeability is not known.

at the tip of the stereocilium. At the base of a 6-μm stereocilium, however, there is no appreciable increase before 10 ms, and steady-state levels are nearly 100 times less. Thus, the site of calcium action is near or at the tips of the stereocilia; it could not reach the base or the cuticular plate in the short time it takes to change the adaptation rate.

**Active Bundle Motion.** Maintained positive displacements of the stereociliary bundle cause the compliance of the bundle to increase with the same time course as adaptation of the transduction current, suggesting that the tension in the elements that act on the transduction channels decreases (5). The voltage dependence of the $I(X)$ curve offers a further test of this hypothesis. If the tension on the channels normally contributes to the equilibrium of forces that maintains the bundle in its rest position, changing this tension by varying membrane potential should perturb the equilibrium and cause an unconstrained bundle to move actively to another position. How much should the bundle move? A simple model assumes that two "springs" dictate bundle position: the pivot point at the base of each stereocilium, and the gating springs, which are assumed to have the same geometry as the "tip links" seen in electron micrographs of hair cells (19). The voltage dependence of the resting $I(X)$ curve (Fig. 4) implies that depolarization increases the tension in the gating springs. For each pair of stereocilia in this model, increased tension would pull the taller stereocilium in the direction of the shorter until that tension is balanced by a restoring force exerted by the pivot spring. It can be shown that this displacement is approximately equal to $K_g/K_s \cdot \Delta X$, where $K_g$ and $K_s$ are spring constants of the gating springs and pivot springs, respectively, and $\Delta X$ is the magnitude of the voltage-dependent $I(X)$ shift, 350 nm in these experiments. $K_s$ has been determined by Howard and Hudspeth (13) to be 440 $\mu N \cdot m^{-1}$; $K_g$ is estimated from the steepness of our $I(X)$ curve to be 49 $\mu N \cdot m^{-1}$. Therefore, the predicted movement is ≈40 nm. In fact, changing membrane potential did produce active bundle movements, which were clearly visible by eye using high-resolution video. In Fig. 7, the membrane potential was initially held at −80 mV and a video image of the bundle was stored. This image was then subtracted from an image stored at +80 mV, so that only differences became visible. When the membrane potential was stepped to +80 mV, the tips of the stereocilia moved, and the difference declined to 0 at their bases, indicating a pivoting motion. No movement was evident in the cuticular plate or cell body. The magnitude of the movement, measured at the tip of the tallest stereocilium, was 22 nm in this cell. Depolarization to +80 mV always caused movement away from the kinocilium. Therefore, both the magnitude and direction of movement are consistent with the model. While we cannot at this point exclude some other voltage-dependent mechanism, it is likely that these movements are driven by tensioning and relaxing of the gating springs.

## DISCUSSION

Our results suggest that calcium must enter the stereocilia to affect adaptation and, furthermore, that calcium's specific site of action is very near the transduction channels through which it enters. (It remains possible that adaptation of the transduction mechanism incorporates several different components, with different time courses. If so, a slow component that was not observed at this time scale could be located elsewhere.)

It has been assumed that the adaptation mechanism serves to set the resting bias on the transduction channels (3, 20). The joint dependence of the adaptation and the resting $I(X)$ curve on calcium and on membrane potential, observed here, is the strongest evidence for this idea. In that regard, it is intriguing that the steepness of the $I(X)$ curves differed at −80

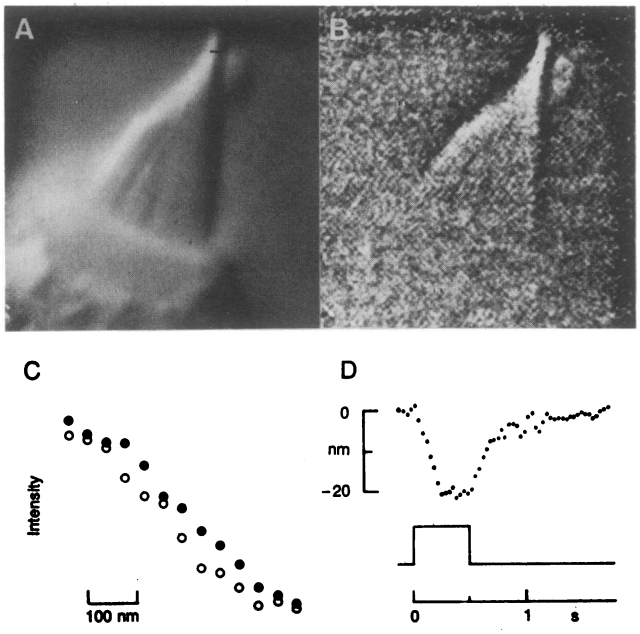


FIG. 7. Voltage-dependent bundle motion. (*A*) High-resolution video Nomarski image of bundle. (*B*) Images at +80 and −80 mV were subtracted to reveal bundle movements. Movements were clearly visible in 8 of 11 cells examined. (*C*) The magnitude and time course of the movements were measured from the video images by measuring the intensity profile of a 0.5-μm 13-pixel horizontal line shown near the tips (+80 mV; ○) and shifting it horizontally to match a reference profile acquired at −80 mV (●). Five cells were suitably oriented in the visual field to allow measurement in this manner. The average movement was 32 ± 14 nm. (*D*) Five cycles of movement were averaged to determine the time course of the motion. Positive displacements (toward the kinocilium, corresponding to putative relaxation of tip-link tension) are shown as upward. Membrane potential time course is shown in the lower trace.

and +80 mV (Fig. 4). It is possible that each gating spring/channel unit in the bundle acts independently, so that a cell's macroscopic $I(X)$ curve is actually the sum of 50 or so microscopic $I(X)$ curves, one for each stereociliary pair. At +80 mV, the units might all assume different set points, causing the overall $I(X)$ curve to broaden, while at −80 mV, adaptation may provide feedback so that a common set point is adopted, tightening the macroscopic $I(X)$ curve.

The active voltage-dependent bundle motions observed in these experiments are consonant with a direct spring-like element communicating tension to the transduction channels: modulating this tension by changing membrane potential moves the bundle to a new position. While additional experiments are clearly necessary to support this hypothesis—for example, it remains to be seen whether the voltage-dependent movements have the same calcium requirement as the voltage-dependent $I(X)$ shift—the results are consistent with the gating springs hypothesis for transduction (4, 18, 19) and with the specific stiffness of each element measured by Howard and Hudspeth (5, 13). Moreover, if these bundle motions are generated by the adaptation mechanism, it implies that the mechanism involves an active energy-consuming motor in the tips of the stereocilia.

Since the movement reported here involves a pivoting of stereocilia about their bases, it is clearly distinct from the voltage-dependent cell-body length changes reported in mammalian outer hair cells (21). It is also apparently unrelated to the oscillations of bundle position that are synchronized with oscillations of membrane potential in turtle cochlear hair cells, as the direction of bundle movement was opposite that reported here (22).

Several other groups have studied hair-cell transduction with whole-cell patch-clamp recording, and it is interesting that none has observed adaptation of this sort. Turtle cochlear hair cells (23) seem not to adapt to maintained displacements. It may be that this process is most vigorous in hair cells of otolith organs. Chicken "vestibular" hair cells also do not show adaptation (9); in that study, it is unclear exactly which vestibular organs were used. Perhaps most surprising is the absence of adaptation in a careful patch-clamp study of bullfrog saccular hair cells (14). These hair cells have been studied with a variety of preparations (3–5); in all others the adaptation was robust. While it is possible that slight technical differences between Holton and Hudspeth's and our experiments could account for the discrepancy, the results are consistent in one sense: Holton and Hudspeth found no adaptation, and they found no voltage dependence of the resting $I(X)$ curve (14). We found both adaptation and voltage dependence in 4 mM extracellular calcium, and neither in 0.1 mM, further suggesting that the adaptation sets the resting bias on the transduction channels. These results suggest that voltage acts only indirectly on both processes, and that the primary modulator of the resting tension on the transduction channels is calcium entering the tips of the stereocilia.

This work was supported by National Institutes of Health Grant NS22059 to D.P.C., a National Science Foundation Predoctoral Fellowship to J.A.A., by the Office of Naval Research, and by the Howard Hughes Medical Institute.

1. Koyama, H., Lewis, E. R., Leverenz, E. L. & Baird, R. A. (1982) *Brain Res.* **250**, 168–172.
2. Corey, D. P. & Hudspeth, A. J. (1983) *J. Neurosci.* **3**, 942–961.
3. Eatock, R. A., Corey, D. P. & Hudspeth, A. J. (1987) *J. Neurosci.* **7**, 2821–2836.
4. Corey, D. P. & Hudspeth, A. J. (1983) *J. Neurosci.* **3**, 962–976.
5. Howard, J. & Hudspeth, A. J. (1987) *Proc. Natl. Acad. Sci. USA* **84**, 3064–3068.
6. Corey, D. P., Smith, W. J., Barres, B. A. & Koroshetz, W. J. (1987) *Soc. Neurosci. Abstr.* **13**, 538.
7. Assad, J. A. & Corey, D. P. (1988) *Biophys. J.* **53**, 429a (abstr.).
8. Lewis, R. S. & Hudspeth, A. J. (1983) *Nature (London)* **304**, 538–541.
9. Ohmori, H. (1985) *J. Physiol. (London)* **359**, 189–217.
10. Corey, D. P. & Hudspeth, A. J. (1980) *J. Neurosci. Methods* **3**, 183–202.
11. Hamill, O. P., Marty, A., Neher, E., Sakmann, B. & Sigworth, F. J. (1981) *Pflügers Arch.* **391**, 85–100.
12. Corey, D. P. & Stevens, C. F. (1983) in *Single-Channel Recording*, eds. Sakmann, B. & Neher, E. (Plenum, New York), pp. 53–68.
13. Howard, J. & Hudspeth, A. J. (1988) *Neuron* **1**, 189–199.
14. Holton, T. & Hudspeth, A. J. (1986) *J. Physiol. (London)* **375**, 195–227.
15. Corey, D. P. & Hudspeth, A. J. (1979) *Nature (London)* **281**, 675–677.
16. Jack, J. J. B., Noble, D. & Tsien, R. W. (1983) *Electric Current Flow in Excitable Cells* (Oxford Univ. Press, Oxford), p. 232.
17. Hudspeth, A. J. & Lewis, R. S. (1988) *J. Physiol. (London)* **400**, 237–274.
18. Hudspeth, A. J. (1982) *J. Neurosci.* **2**, 1–10.
19. Pickles, J. O., Comis, S. D. & Osborne, O. P. (1984) *Hearing Res.* **15**, 103–112.
20. Howard, J. & Hudspeth, A. J. (1987) *Discuss. Neurosci.* **4**, 138–145.
21. Brownell, W. E., Bader, C. R., Bertrand, D. & de Ribaupierre, Y. (1985) *Science* **227**, 194–196.
22. Crawford, A. C. & Fettiplace, R. (1985) *J. Physiol. (London)* **364**, 359–379.
23. Art, J. J., Crawford, A. C. & Fettiplace, R. (1986) in *Auditory Frequency Selectivity*, eds. Moore, B. C. J. & Patterson, R. D. (Plenum, New York), pp. 81–88.